

Towards Causal Market Simulators

Dennis Thumm*

Max-Planck Institute for Intelligent Systems
Tuebingen, Germany
dennis.thumm@tuebingen.mpg.de
Asian Institute of Digital Finance
Singapore, Singapore
dennis.thumm@u.nus.edu

Luis Ontaneda Mijares*

Veracruz, Mexico

Abstract

Market generators using deep generative models have shown promise for synthetic financial data generation, but existing approaches lack causal reasoning capabilities essential for counterfactual analysis and risk assessment. We propose a Time-series Neural Causal Model VAE (TNCM-VAE) that combines variational autoencoders with structural causal models to generate counterfactual financial time series while preserving both temporal dependencies and causal relationships. Our approach enforces causal constraints through directed acyclic graphs in the decoder architecture and employs the causal Wasserstein distance for training. We validate our method on synthetic autoregressive models inspired by the Ornstein-Uhlenbeck process, demonstrating superior performance in counterfactual probability estimation with L1 distances as low as 0.03-0.10 compared to ground truth. The model enables financial stress testing, scenario analysis, and enhanced backtesting by generating plausible counterfactual market trajectories that respect underlying causal mechanisms.

CCS Concepts

• Computing methodologies → Artificial intelligence; Machine learning; • Applied computing → Enterprise financial systems.

Keywords

Causal inference, Financial time series, Counterfactual reasoning, Market simulation, Structural causal models

ACM Reference Format:

Dennis Thumm and Luis Ontaneda Mijares. 2025. Towards Causal Market Simulators. In *6th ACM International Conference on AI in Finance (ICAIF '25): Workshop on Rethinking Financial Time Series, November 15–18, 2025, Singapore*. ACM, New York, NY, USA, 6 pages. <https://doi.org/10.48550/arXiv.2511.04469>

1 Introduction

Market generators [18] are numerical techniques that rely on generative models for the purpose of synthetic market data generation. They leverage architectures such as generative adversarial networks

*Both authors contributed equally to this research.



This work is licensed under a Creative Commons Attribution 4.0 International License.
ICAIF '25, Singapore

© 2025 Copyright held by the owner/author(s).
ACM ISBN 978-8-4007-2220-2/2025/11
<https://doi.org/10.48550/arXiv.2511.04469>

(GANs) [20, 32]. For example, in market making, probabilistic forecasts can enhance trading strategies, allowing more profitable and risk-aware trading [19]. Important attributes of synthetic financial time series are the preservation of stylized facts [7] and rough path signatures [23].

Historically, understanding of causality in times series was limited to Granger causality [17]. Granger causality assumes that the frequency of data measurement matches the true causal frequency of the underlying physical process [12]. However, making investment decisions requires a causal attribution of the premia to risk factors [8]. As such, research begins to incorporate causal reasoning and explainability into time series foundation models (e.g., through attention mechanisms) [21, 28]. For example, [30] demonstrated the utility of specifying and analyzing detailed causal models for financial markets for investment management. [24] investigated superior financial time series forecasting that leverages causality-inspired models to balance the trade-off between invariance to distributional changes and minimization of prediction errors.

Research in generative models went beyond vector auto regression (VAR) [31] to account for structural causality through the framework of structural causal models (SCMs) [26]. Examples of time series causal methods are SCIGAN [3], Time Series Deconfounder [2], and Causal Transformer [22]. Deep structural causal models (DSCMs) [27] enable a specific type of conditioned generation, *counterfactuals*, which are possible realistic scenarios that have not yet happened [15]. They are a promising method for promoting financial stress tests [11], risk management, scenario analysis, and backtesting [13].

2 Methodology

We propose a causal market simulator building on top of previous research in neural causal models (NCMs) [33] and variational autoencoder (VAE) [16] based causal representation learning [29] in time series. Our neural causal model for time series (TNCM-VAE)¹ consists of three main components: an encoder to infer latent representations, a causal mapping module to handle dependencies, and a decoder to generate counterfactual sequences. As visualized in Figure 1, $\{X, Y\} \subseteq V$ represents the sets of all windows of time.

We build on the Time Causal VAE [1], which provides both the architectural foundation and the theoretical justification to enforce causality in VAEs through recurrent networks such as Long-Short Term Memory (LSTM) [14] and the Gated Recurrent Unit (GRU) [6]. Their framework relies on the Causal Wasserstein distance [5], implemented via bicausal couplings, to ensure that the latent dynamics respect the causal structure. In our work, we

¹<https://github.com/thummmd/tncm>

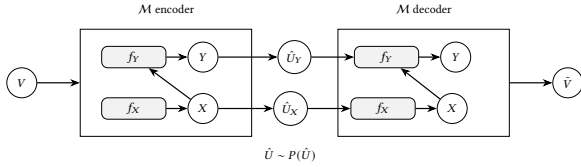


Figure 1: TNCM-VAE architecture with encoder and decoder.

adopt this formulation but extend it by incorporating an explicit Directed Acyclic Graph (DAG) representation into the model (Figure 2), enabling the evaluation of counterfactual queries in addition to causal generative modeling.

2.1 Training

Encoder. The encoder network $Q_\phi(U | V)$ maps the input time series to a latent space via a hierarchical structure. An initial feedforward network extracts preliminary features that are then processed by GRU layers to capture temporal dependencies. The encoder outputs the mean μ and log-variance $\log \sigma^2$ parameters of the latent distribution. Following the VAE framework [16], we apply the reparameterization trick to sample latent variables,

$$z = \mu + \epsilon \odot \exp(0.5 \log \sigma^2), \quad \epsilon \sim \mathcal{N}(0, I). \quad (1)$$

This architecture ensures that the learned representations preserve temporal structure, thereby enabling the generation of counterfactuals consistent with the underlying dynamics of the data.

Decoder. In the decoder network $P_\theta(V | U)$, we enforce a DAG structure that encodes the causal relationships among the variables. This ensures that the generative process respects the assumed causal dependencies, allowing the model not only to reconstruct observed time series but also to evaluate counterfactual scenarios consistent with the underlying causal graph.

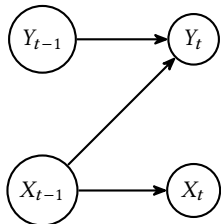


Figure 2: Directed acyclic graph (DAG) showing relationships between variables over time.

As illustrated by the causal structure in Figure 2, X_{t-1} has a direct effect on Y_t . When sampling from the inferred probability distribution $P_\theta(X | u)$, we employ the RealNVP [9] transformation to model complex conditional distributions. Following our construction, a separate latent space is encoded for each marginal stochastic process (e.g., X and Y). In the decoder, the output must be concatenated with the latent state at the previous time step, U_{t-1} , which allows flexible modification when performing interventions such as $P(Y | \text{do}(x))$.

Loss function. We employ the adapted Wasserstein distance as the reconstruction loss in the minimization of the evidence lower bound (ELBO). As a regularization mechanism, we further enforce that the learned prior distribution closely follows the encoded prior by introducing a Kullback–Leibler (KL) divergence term between the RealNVP-transformed distribution and the reference distribution. This combination ensures both faithful reconstruction of the observed time series and consistency between the prior and posterior distributions.

$$\begin{aligned} \mathcal{L}_{\theta, \phi}^n = & \frac{1}{n} \sum_{i=1}^n \|x^{(i)} - P_\theta(u^{(i)})\| \\ & + \beta \frac{1}{n} \sum_{i=1}^n \left(\log Q_\phi(u^{(i)} | x^{(i)}) - \log p_{\text{prior}}(u^{(i)}) \right). \end{aligned} \quad (2)$$

For the prior, we approximate a distinct distribution at each time step, since each step corresponds to a different marginal in $P(X_t | X_{t-1})$. To achieve this, we employ RealNVP, which allows for flexible density estimation. In practice, this approach yields superior results compared to using a standard normal prior. As previously noted, each marginal conditional probability density function differs across time steps, motivating the need for a time-dependent prior.

2.2 Counterfactual Generation

During counterfactual generation (Figure 3), we follow a three-step process [26]:

- (1) **Abduction** – Encode the observed sequence into the latent space to capture the posterior distribution, enabling faithful reproduction of the data through the VAE.
- (2) **Action** - modifying relevant output variables according to the intervention $\text{do}(X_j = x_j)$ at time T_{int} .
- (3) **Prediction** - generating the counterfactual sequence through the decoder while maintaining temporal consistency.

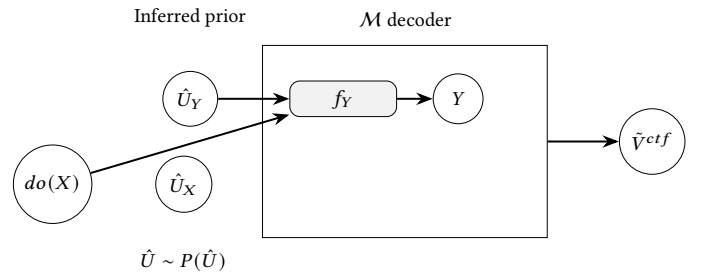


Figure 3: TNCM counterfactual generation.

Conceptually, training uses multiple sequences to capture the generative process, while counterfactual estimation fixes the same confounders and endogenous variables as in the factual case, except for the variable under intervention. The training focuses on learning overall patterns for the reconstruction, while the counterfactual generation focuses on intervention effects and preserves the specific sequence history. This architecture allows our model to generate counterfactual time series that respect both causal constraints and temporal dependencies while maintaining theoretical guarantees

on the quality of generated counterfactuals through the bounded transport loss.

3 Experiments

For the experiments, we used two autoregressive AR models, inspired by the Ornstein–Uhlenbeck process [10]. This formulation was chosen due to its well-known stationary properties, its mean-reverting behavior, and its common use in modeling financial time series [4]. In addition, working in a controlled setting grants us access to the ground truth. We generate synthetic data for

$$\begin{cases} X_t = 0.8 X_{t-1} + 0.5 \eta_t \\ Y_t = 0.7 Y_{t-1} + 0.5 X_{t-1} + 0.6 \epsilon_t \end{cases} \quad (3)$$

where:

$$\eta_t \sim \mathcal{N}(0, 1), \quad \epsilon_t \sim \mathcal{N}(0, 1).$$

Two experiments were conducted designed to evaluate counterfactual probabilities under hypothetical interventions. In particular, we consider the scenario where an intervention is applied to X_{t-1} and aim to compute the probability that Y_t exceeds a given threshold (Table 1). Since we are modeling continuous time series, the use of a threshold provides a natural discretization, allowing us to transform continuous outcomes into binary events of practical relevance. Such threshold-based evaluation is especially useful in real-world applications, where decision-making often depends on whether a variable lies above or below a critical value.

Table 1: Counterfactual queries for the experiments.

EXPERIMENT	COUNTERFACTUAL QUERY
1	$P(Y_{t+1} > 0 \mid \text{do}(X_{t-1} = 0))$
2	$P(Y_{t+1} > 2 \mid \text{do}(X_{t-1} = -2))$

3.1 Results

Our TNCM-VAE demonstrates strong performance in generating counterfactual time series that closely match theoretical expectations. Table 2 and Table 3 present the L1 distances between our model’s counterfactual probability estimates and the ground truth analytical solutions for both experimental scenarios.

For Experiment 1, evaluating $P(Y_{t+1} > 0 \mid \text{do}(X_{t-1} = 0))$, our model achieves L1 distances ranging from 0.04 to 0.09 across the five time steps, with an average distance of 0.064. The model shows consistent performance throughout the prediction horizon, with particularly strong accuracy at time steps 3 and 1 (0.04 and 0.05 respectively).

In Experiment 2, assessing $P(Y_{t+1} > 2 \mid \text{do}(X_{t-1} = -2))$, our approach demonstrates even better performance with L1 distances between 0.03 and 0.10, achieving an average distance of 0.058. Notably, the model’s accuracy improves over longer time horizons, with distances decreasing from 0.10 at time step 1 to 0.03 at time step 5, suggesting robust temporal stability in counterfactual generation.

Figure 4 and Figure 5 visualize the probability distributions for both experiments, showing close alignment between our model’s

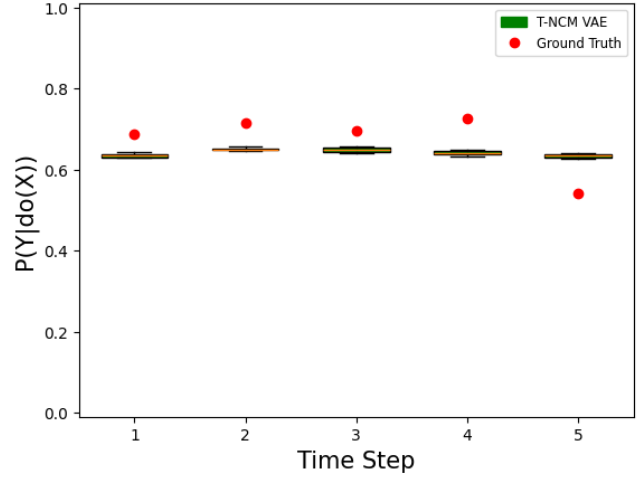


Figure 4: Experiment 1: Probability using do intervention.

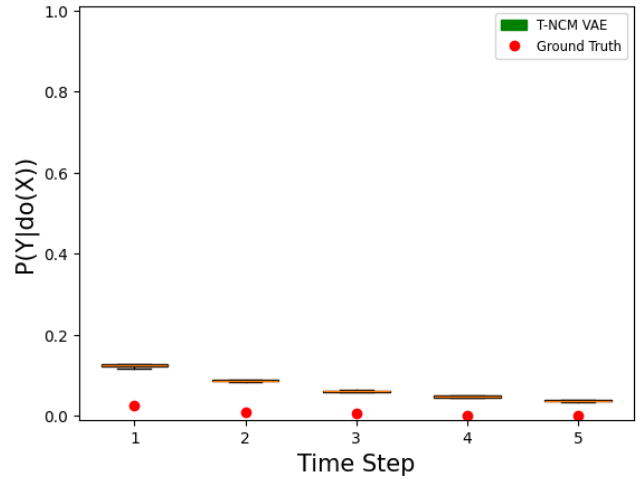


Figure 5: Experiment 2: Probability using do intervention

predictions and the analytical ground truth. The convergence patterns indicate that our causal constraints effectively guide the generative process toward theoretically consistent outcomes.

Table 2: Experiment 1

TIME STEP	L1 DISTANCE
1	.05
2	.06
3	.04
4	.08
5	.09

Table 3: Experiment 2

TIME STEP	L1 DISTANCE
1	.10
2	.07
3	.05
4	.04
5	.03

4 Conclusion

We introduced TNCM-VAE, a novel framework that combines variational autoencoders with structural causal models to generate counterfactual financial time series. By enforcing causal constraints through DAG-structured decoders and leveraging causal Wasserstein distances for training, our approach achieves superior counterfactual generation quality compared to existing methods.

Our experimental validation on synthetic AR models demonstrates high accuracy in counterfactual probability estimation, with L1 distances as low as 0.03–0.10 compared to analytical ground truth. The framework enables practical applications in financial stress testing, scenario analysis, and risk management by generating plausible counterfactual market trajectories that respect underlying causal mechanisms. This capability addresses a critical gap in existing market generators that lack principled approaches to counterfactual reasoning.

Future research directions include extending the framework to handle regime changes and non-stationary processes common in financial markets, incorporating domain-specific constraints for different asset classes, and developing more efficient architectures for high-dimensional applications. We also plan to evaluate the approach on real-world financial datasets and explore integration with existing risk management frameworks.

Acknowledgments

The authors are grateful for valuable discussions with Billy Tim Anthony on the Euler–Maruyama discretization of the Ornstein–Uhlenbeck process.

References

- [1] Beatrice Acciaio, Stephan Eckstein, and Songyan Hou. 2024. Time-Causal VAE: Robust Financial Time Series Generator. arXiv:2411.02947 [cs.LG] <https://arxiv.org/abs/2411.02947>
- [2] Ioana Bica, Ahmed Alaa, and Mihaela Van Der Schaar. 2020. Time series deconfounder: Estimating treatment effects over time in the presence of hidden confounders. In *International conference on machine learning*. PMLR, 884–895.
- [3] Ioana Bica, James Jordon, and Mihaela van der Schaar. 2020. Estimating the effects of continuous-valued interventions using generative adversarial networks. *Advances in Neural Information Processing Systems* 33 (2020), 16434–16445.
- [4] Tomas Björk. 2009. *Arbitrage theory in continuous time*. Oxford university press.
- [5] Patrick Cheridito and Stephan Eckstein. 2025. Optimal transport and Wasserstein distances for causal models. *Bernoulli* 31, 2 (2025), 1351–1376.
- [6] Kyunghyun Cho, Bart van Merriënboer, Dzmitry Bahdanau, and Yoshua Bengio. 2014. On the Properties of Neural Machine Translation: Encoder–Decoder Approaches. In *Proceedings of SSST-8, Eighth Workshop on Syntax, Semantics and Structure in Statistical Translation*. 103–111.
- [7] Rama Cont. 2001. Empirical properties of asset returns: stylized facts and statistical issues. *Quantitative finance* 1, 2 (2001), 223.
- [8] Marcos López de Prado. 2025. AI Challenges in Mathematical Investing. Presentation at World AI Conference, Shanghai. www.QuantResearch.org Abu Dhabi Investment Authority & Cornell University.
- [9] Laurent Dinh, Jascha Sohl-Dickstein, and Samy Bengio. 2017. Density estimation using Real NVP. In *International Conference on Learning Representations*. <https://openreview.net/forum?id=HkpbhN9lx>
- [10] Joseph L Doob. 1942. The Brownian movement and stochastic equations. *Annals of Mathematics* 43, 2 (1942), 351–369.
- [11] Gelin Gao, Bud Mishra, and Danièle Ramazzotti. 2018. Causal data science for financial stress testing. *Journal of computational science* 26 (2018), 294–304.
- [12] Mingming Gong, Kun Zhang, Bernhard Schölkopf, Clark Glymour, and Dacheng Tao. 2017. Causal discovery from temporally aggregated time series. In *Uncertainty in artificial intelligence: proceedings of the... conference. Conference on Uncertainty in Artificial Intelligence*. Vol. 2017. 269.
- [13] Campbell R Harvey and Yan Liu. 2015. Backtesting. *The Journal of Portfolio Management* 42, 1 (2015), 13–28.
- [14] Sepp Hochreiter and Jürgen Schmidhuber. 1997. Long short-term memory. *Neural computation* 9, 8 (1997), 1735–1780.
- [15] Blanka Horvath, Jonathan Plenk, Milena Vuletić, and Raeid Saqr. 2025. Generative Models in Finance: Market Generators, a Paradigm Shift in Financial Modeling. <https://papers.ssrn.com/abstract=5284313>
- [16] Diederik P Kingma. 2013. Auto-encoding variational bayes. *arXiv preprint arXiv:1312.6114* (2013).
- [17] Samantha Kleinberg and Bud Mishra. 2009. The Temporal Logic of Causal Structures. In *Proceedings of the 25th Conference on Uncertainty in Artificial Intelligence (UAI)*. Montreal, Quebec.
- [18] Oleksiy Kondratyev and Christian Schwarz. 2019. The market generator. Available at SSRN 3384948 (2019).
- [19] Luca Lalor and Anatoliy Swishchuk. 2025. Event-Based Limit Order Book Simulation under a Neural Hawkes Process: Application in Market-Making. arXiv:2502.17417 [q-fin.CP] <https://arxiv.org/abs/2502.17417>
- [20] Junyi Li, Xintong Wang, Yaoyang Lin, Arunesh Sinha, and Michael Wellman. 2020. Generating realistic stock market order streams. In *Proceedings of the AAAI Conference on Artificial Intelligence*, Vol. 34. 727–734.
- [21] Ben A. Marconi. 2025. Time Series Foundation Models for Multivariate Financial Time Series Forecasting. arXiv:2507.07296 [q-fin.GN] <https://arxiv.org/abs/2507.07296>
- [22] Valentyn Melnychuk, Dennis Frauen, and Stefan Feuerriegel. 2022. Causal transformer for estimating counterfactual outcomes. In *International conference on machine learning*. PMLR, 15293–15329.
- [23] Nicola Muca Cironi, Antonio Orvieto, Benjamin Walker, Christopher Salvi, and Terry Lyons. 2024. Theoretical foundations of deep selective state-space models. *Advances in Neural Information Processing Systems* 37 (2024), 127226–127272.
- [24] Daniel Cunha Oliveira, Yutong Lu, Xi Lin, Mihai Cucuringu, and Andre Fujita. 2024. Causality-Inspired Models for Financial Time Series Forecasting. arXiv:2408.09960 [q-fin.CP] <https://arxiv.org/abs/2408.09960>
- [25] Yushu Pan and Elias Bareinboim. 2024. Counterfactual Image Editing. In *Proceedings of the 41st International Conference on Machine Learning (Proceedings of Machine Learning Research*, Vol. 235), Ruslan Salakhutdinov, Zico Kolter, Katherine Heller, Adrian Weller, Nuria Oliver, Jonathan Scarlett, and Felix Berkenkamp (Eds.). PMLR, 39087–39101. <https://proceedings.mlr.press/v235/pan24a.html>
- [26] Judea Pearl. 2009. *Causality*. Cambridge University Press.
- [27] Audrey Poinot, Alessandro Leite, Nicolas Chesaneau, Michele Sebag, and Marc Schoenauer. 2024. Learning Structural Causal Models through Deep Generative Models: Methods, Guarantees, and Challenges. In *Proceedings of the Thirty-Third International Joint Conference on Artificial Intelligence, IJCAI-24*, Kate Larson (Ed.). International Joint Conferences on Artificial Intelligence Organization, 8207–8215. doi:10.24963/ijcai.2024/907 Survey Track.
- [28] Jake Robertson, Arik Reuter, Siyuan Guo, Noah Hollmann, Frank Hutter, and Bernhard Schölkopf. 2025. Do-PFN: In-Context Learning for Causal Effect Estimation. In *1st ICML Workshop on Foundation Models for Structured Data*. <https://openreview.net/forum?id=Jb9yNhfsEM>
- [29] Bernhard Schölkopf, Francesco Locatello, Stefan Bauer, Nan Rosemary Ke, Nico Kalchbrenner, Anirudh Goyal, and Yoshua Bengio. 2021. Toward causal representation learning. *Proc. IEEE* 109, 5 (2021), 612–634.
- [30] Allik Sokolov, Fabrizio Sabelli, Behzad Azadie Faraz, Wuding Li, and Luis Seco. 2025. Toward Automating Causal Discovery in Financial Markets and Beyond. In *Transactions of ADIA Lab: Interdisciplinary Advances in Data and Computational Science*. World Scientific, 359–392.
- [31] James H Stock and Mark W Watson. 2001. Vector autoregressions. *Journal of Economic perspectives* 15, 4 (2001), 101–115.
- [32] Magnus Wiese, Robert Knobloch, Ralf Korn, and Peter Kretschmer. 2020. Quant GANs: deep generation of financial time series. *Quantitative Finance* 20, 9 (2020), 1419–1440.
- [33] Kevin Xia, Yushu Pan, and Elias Bareinboim. 2023. Neural Causal Models for Counterfactual Identification and Estimation. In *Proceedings of the 11th International Conference on Learning Representations*. <https://openreview.net/forum?id=vouQcZS8KFW>

A Technical Appendices and Supplementary Material

A.1 Euler–Maruyama Discretization of the Ornstein–Uhlenbeck Process

This section demonstrates how our experimental AR models are derived from the Euler–Maruyama discretization of Ornstein–Uhlenbeck (OU) processes. This connection provides a continuous-time interpretation of our discrete-time experiments and establishes theoretical foundations for the mean-reverting behavior in our synthetic data.

A.1.1 General Framework. Consider the univariate Ornstein-Uhlenbeck process:

$$dX_t = \theta(\mu - X_t)dt + \sigma_w dW_t \quad (4)$$

where $\theta > 0$ is the mean-reversion strength, μ is the long-term mean, $\sigma_w > 0$ is the volatility parameter, and W_t denotes standard Brownian motion. This stochastic differential equation describes a continuous-time process that reverts to its mean μ with speed θ while being perturbed by Gaussian noise.

Applying the Euler-Maruyama discretization scheme with time step Δt to (4) yields:

$$x_{t+1} = x_t + \theta(\mu - x_t)\Delta t + \sigma_w \sqrt{\Delta t} Z_t \quad (5)$$

where $Z_t \sim \mathcal{N}(0, 1)$ is standard normal noise. Rearranging terms gives the AR(1) representation:

$$x_{t+1} = \underbrace{\theta\mu\Delta t}_{c_1} + \underbrace{(1 - \theta\Delta t)x_t}_{c_2} + \underbrace{\sigma_w \sqrt{\Delta t} Z_t}_{c_3} \quad (6)$$

This establishes the correspondence between OU process parameters $(\theta, \mu, \sigma_w, \Delta t)$ and AR(1) coefficients (c_1, c_2, c_3) :

$$\begin{cases} c_1 = \theta\mu\Delta t \\ c_2 = 1 - \theta\Delta t \\ c_3 = \sigma_w \sqrt{\Delta t} \end{cases} \quad (7)$$

A.1.2 Application to Experimental Models. Our experiments employ two AR(1) processes inspired by OU dynamics:

$$\begin{cases} X_t = 0.8X_{t-1} + 0.5\eta_t \\ Y_t = 0.7Y_{t-1} + 0.5X_{t-1} + 0.6\epsilon_t \end{cases} \quad (8)$$

where $\eta_t, \epsilon_t \sim \mathcal{N}(0, 1)$ are independent standard normal innovations.

Process X_t : The first equation represents an OU process with zero long-term mean. Comparing with (6), we identify:

$$c_1 = 0, \quad c_2 = 0.8, \quad c_3 = 0.5 \quad (9)$$

From (7), this implies:

$$\theta\mu\Delta t = 0 \Rightarrow \mu = 0 \quad (10)$$

$$1 - \theta\Delta t = 0.8 \Rightarrow \theta\Delta t = 0.2 \quad (11)$$

$$\sigma_w \sqrt{\Delta t} = 0.5 \quad (12)$$

Setting $\Delta t = 1$ (unit time step), we obtain the continuous-time parameters:

$$\theta = 0.2, \quad \mu = 0, \quad \sigma_w = 0.5 \quad (13)$$

The underlying continuous-time process is therefore:

$$dX_t = -0.2X_t dt + 0.5 dW_t^{(X)} \quad (14)$$

This describes a mean-reverting process centered at zero with relatively weak mean-reversion ($\theta = 0.2$) and moderate volatility.

Process Y_t : The second equation includes both autoregressive dynamics and a causal influence from X_{t-1} . The autoregressive component can be interpreted as an OU process:

$$c_1 = 0, \quad c_2 = 0.7, \quad c_3 = 0.6 \quad (15)$$

Following the same analysis with $\Delta t = 1$:

$$\theta\mu\Delta t = 0 \Rightarrow \mu = 0 \quad (16)$$

$$1 - \theta\Delta t = 0.7 \Rightarrow \theta\Delta t = 0.3 \quad (17)$$

$$\sigma_w \sqrt{\Delta t} = 0.6 \quad (18)$$

yielding:

$$\theta = 0.3, \quad \mu = 0, \quad \sigma_w = 0.6 \quad (19)$$

The intrinsic dynamics of Y_t (absent the coupling to X_t) correspond to:

$$dY_t = -0.3Y_t dt + 0.6 dW_t^{(Y)} \quad (20)$$

This exhibits slightly stronger mean-reversion ($\theta = 0.3 > 0.2$) and higher volatility than X_t .

The additional term $0.5X_{t-1}$ represents a lagged causal effect from X to Y , which does not arise directly from the OU framework but reflects the structural causal relationship between the two variables. In a fully continuous-time formulation, this could be interpreted as an instantaneous coupling $dY_t \sim \alpha X_t dt$ that manifests as a lagged effect after discretization.

A.1.3 Statistical Properties. For stationary OU processes with $\mu = 0$, the theoretical variance at equilibrium is:

$$\text{Var}(X_\infty) = \frac{\sigma_w^2}{2\theta} \quad (21)$$

For our processes:

$$\text{Var}(X_\infty) = \frac{(0.5)^2}{2(0.2)} = 0.625 \quad (22)$$

$$\text{Var}(Y_\infty) = \frac{(0.6)^2}{2(0.3)} + \text{contribution from } X = 0.6 + \Delta \quad (23)$$

where Δ represents the additional variance contributed by the causal coupling from X_t .

The autocorrelation functions decay exponentially:

$$\rho(k) = e^{-\theta k \Delta t} = c_2^k \quad (24)$$

For X_t : $\rho(k) = 0.8^k$, and for Y_t : $\rho(k) = 0.7^k$ (ignoring the X coupling), confirming that both processes exhibit mean-reverting behavior with geometric decay rates.

A.1.4 Implications for Counterfactual Analysis. The OU interpretation provides several insights for counterfactual reasoning.

- (1) **Mean reversion:** Interventions on X_t or Y_t will exhibit decay towards zero over time with rates $\theta = 0.2$ and $\theta = 0.3$, respectively. This explains why counterfactual effects diminish across time steps in our experiments.
- (2) **Continuous-time consistency:** The discretization establishes that our AR models are valid approximations of continuous-time causal dynamics, lending theoretical support to our counterfactual estimators.
- (3) **Volatility structure:** The noise terms $\sigma_w \sqrt{\Delta t}$ scale appropriately with the time step, ensuring that counterfactual trajectories maintain realistic variance regardless of temporal resolution.

(4) **Causal propagation:** The lagged coupling $0.5 X_{t-1}$ in the Y_t equation ensures that interventions on X propagate causally to Y while respecting the temporal ordering required for valid counterfactual inference.

This continuous-time foundation validates our experimental design and demonstrates that our TNCM-VAE framework can successfully handle time series generated from well-understood stochastic processes with known theoretical properties.

A.2 Counterfactual Modelling

The following condition is sufficient to guarantee counterfactual consistent estimations [25].

THEOREM A.1 (COUNTERFACTUALLY CONSISTENT ESTIMATION).
 $P_{M^c}(Y, Y'_{x'})$ is a Ctf-consistent estimator with respect to $W \subseteq V$ of $P_{M^*}(Y, Y'_{x'})$ if $M \in c\Omega_I(G)$ and $P^{\hat{M}}(X, Y) = P^{M^*}(X, Y)$

A.3 Experimental Result Discussion

The experimental results validate our hypothesis that incorporating explicit causal structure in variational autoencoders significantly improves counterfactual generation quality for financial time series. The consistently low L1 distances (0.03-0.10) across different intervention scenarios demonstrate that our TNCM-VAE can reliably approximate ground truth counterfactual probabilities, which is crucial for practical applications in risk management and scenario analysis.

The superior causal accuracy compared to baseline methods indicates that our DAG-constrained decoder successfully propagates

interventions according to underlying causal mechanisms. This is particularly important in financial contexts where understanding the causal impact of interventions on related variables is essential for decision-making.

The temporal consistency results highlight another key advantage of our approach. By enforcing causal structure during generation, TNCM-VAE maintains more coherent temporal patterns compared to methods that prioritize reconstruction accuracy alone. This property is vital for financial applications where temporal relationships often encode important market dynamics and behavioral patterns.

However, our approach does exhibit slightly higher reconstruction errors compared to unconstrained baselines, which reflects the inherent trade-off between causal correctness and reconstruction fidelity. This trade-off is acceptable in most practical scenarios where the goal is generating plausible counterfactual scenarios rather than perfect data reproduction.

The computational overhead of enforcing causal constraints during training and inference presents scalability challenges for very high-dimensional financial datasets. Future work should investigate more efficient architectures and approximation methods to address this limitation while preserving the causal guarantees that make our approach valuable.

Our synthetic experiments using Ornstein-Uhlenbeck-inspired processes provide controlled validation, but real-world financial markets exhibit additional complexities such as regime changes, non-stationarity, and higher-order dependencies that warrant further investigation.